



**Providing Choice & Value**

Generic CT and MRI Contrast Agents



CONTACT REP

**AJNR**

**Quantification of Collateral Supply with  
Local-AIF Dynamic Susceptibility Contrast  
MRI Predicts Infarct Growth**

Mira M. Liu, Niloufar Saadat, Steven P. Roth, Marek A. Niekrasz, Mihai Giurcanu, Timothy J. Carroll and Gregory A. Christoforidis

This information is current as  
of July 31, 2025.

*AJNR Am J Neuroradiol* published online 12 August 2024  
<http://www.ajnr.org/content/early/2025/01/02/ajnr.A8441>

# Quantification of Collateral Supply with Local-AIF Dynamic Susceptibility Contrast MRI Predicts Infarct Growth

 Mira M. Liu, Niloufar Saadat, Steven P. Roth,  Marek A. Niekrasz, Mihai Giurcanu,  Timothy J. Carroll, and  Gregory A. Christoforidis



## ABSTRACT

**BACKGROUND AND PURPOSE:** In ischemic stroke, leptomeningeal collaterals can provide delayed and dispersed compensatory blood flow to tissue-at-risk despite an occlusion and can impact treatment response and infarct growth. The purpose of this work is to test the hypothesis that the inclusion of this delayed and dispersed flow with an appropriately calculated local arterial input function (local-AIF) is needed to quantify the degree of collateral blood supply in tissue distal to an occlusion.

**MATERIALS AND METHODS:** Seven experiments were conducted in a preclinical middle cerebral artery occlusion model. Dynamic susceptibility contrast MRI was imaged and postprocessed to yield quantitative cerebral blood flow (qCBF) maps with both a traditionally chosen single arterial input function applied globally to the whole brain (ie, “global-AIF”) and a delay and dispersion corrected AIF (ie, “local-AIF”) that is sensitive to retrograde flow. Leptomeningeal collateral arterial recruitment was quantified with a pial collateral score from x-ray angiograms, and infarct growth was calculated from serially acquired diffusion-weighted MRI scans.

**RESULTS:** The degree of collateralization at x-ray correlated more strongly with local-AIF qCBF in the ischemic penumbra ( $R^2 = 0.81$ ) than with traditional global-AIF qCBF ( $R^2 = 0.05$ ). Local-AIF qCBF was negatively correlated with infarct growth (slower infarct progression with higher perfusion,  $R^2 = 0.79$ ) more strongly than global-AIF qCBF ( $R^2 = 0.02$ ).

**CONCLUSIONS:** In acute stroke, qCBF calculated with a local-AIF is more accurate for assessing tissue status and collateral supply than traditionally chosen global-AIFs. These findings support the use of a local-AIF that corrects for delayed and dispersed retrograde flow in determining quantitative tissue perfusion with collateral supply in occlusive disease.

**ABBREVIATIONS:** AIF = arterial input function; Gd = gadolinium; IVIM = intravoxel incoherent motion; MCAO = middle cerebral artery occlusion; MD = mean diffusivity; PCS = pial collateral score; qCBF = quantitative cerebral blood flow; rCBF = relative cerebral blood flow; Tmax = time-to-maximum

In acute ischemic stroke, where a major blood vessel feeding the brain becomes occluded, it is well-known that the development of compensatory blood flow through the leptomeningeal collateral arterial network (collateral supply) can maintain blood to tissue-at-risk and slow the growth of an infarction of tissue. Minimizing “door-to-needle time” between hospital arrival and treatment currently drives ischemic stroke triage/treatment protocols regardless of an individual’s collateral supply. However,

neuroprotection/bridge therapies, which enhance collateral supply for “drip-and-ship” cases before transfer for specialized intervention, and “wake-up strokes”<sup>1</sup> with unknown time of onset, may benefit from accurate quantification of collateral supply.<sup>2</sup> Further, the patient-to-patient variability of collateral supply contributes to unwanted variability of perfusion-diffusion mismatch, a measure used to predict positive outcomes in patients undergoing thrombectomy.<sup>3</sup> Previous studies have observed a slowing of infarct growth with flow augmentation therapies<sup>4,5</sup> and that the benefit of flow augmentation may be reduced in a setting of robust collateralization.<sup>6,7</sup> Accurate quantification of collateral supply may identify if blood supply is sufficient to maintain viability, determine if blood supply can be therapeutically enhanced to serve as a “bridge” to thrombectomy and provide a more accurate prediction of infarct growth.

Collateral supply can be estimated by x-ray digital subtraction angiography, single-photon emission CT perfusion, CT perfusion, and MR perfusion<sup>1</sup> via prolonged time-to-maximum (Tmax)<sup>8</sup> from DSC. However, difficulties measuring perfusion as absolute

Received June 6, 2024; accepted after revision July 30.

From the Departments of Radiology Medical Physics (M.M.L., T.J.C.), Interventional Radiology (N.S., G.A.C.), Anesthesiology (S.P.R.), Surgery and Large Animal Studies (M.A.N.), and Statistics (M.G.), University of Chicago, Chicago, Illinois; Biomedical Engineering and Imaging Institute (M.M.L.), Icahn School of Medicine at Mount Sinai, New York, New York; and Mount Carmel Health Systems (G.A.C.), Columbus, Ohio.

This work was supported by the US National Institutes of Health R01-NS093908 (Carroll/Christoforidis) and The National Science Foundation DGE-1746045 (Liu).

Please address correspondence to Mira M. Liu, Icahn School of Medicine at Mount Sinai, Biomedical Engineering and Imaging Institute, 1470 Madison Ave, 1st Floor, New York, NY 10029; e-mail: Liusarkarm@uchicago.edu

 Indicates article with online supplemental data.

<http://dx.doi.org/10.3174/ajnr.A8441>

## SUMMARY

**PREVIOUS LITERATURE:** In acute ischemic stroke, the development of compensatory blood flow through the leptomeningeal collateral arterial network can maintain blood to tissue-at-risk and slow the growth of an infarction of tissue. Further, success of flow augmentation to serve as a bridge to thrombectomy may be dependent on leptomeningeal collateralization. Difficulties in measuring blood flow in acute ischemic stroke with a traditional single global-AIF DSC include overestimation of perfusion deficits and failure to include delayed and dispersed compensatory blood flow.

**KEY FINDINGS:** Local-AIF DSC that incorporated delayed and dispersed flow improved correlation of penumbral perfusion against collateral supply at x-ray and against infarct growth compared with global-AIF DSC. Local-AIF is an important correction in DSC of acute stroke to include compensatory collateral perfusion distal to an occlusion, even for relative perfusion.

**KNOWLEDGE ADVANCEMENT:** These findings support the use of a local-AIF rather than a single global-AIF to 1) calculate quantitative cerebral blood flow in tissue-at-risk, 2) reduce false hypoperfusion in DSC of large vessel occlusions, and 3) quantify the blood supplied to a compromised perfusion bed through the leptomeningeal arteries.

CBF with traditional DSC include highly variable compensatory vasodilation of CBV<sup>9</sup> and deconvolution of a traditionally chosen single global arterial input function (global-AIF), overestimating perfusion deficits.<sup>10</sup> While using global-AIF assumes a more uniform input function for ease of computation, the use of a more complex local-AIF allows one to correct for the delay and dispersion of the contrast bolus in every voxel when calculating CBF, thereby providing a more accurate map of CBF.

This study investigates if quantitative cerebral blood flow (qCBF), calculated by using a local-AIF, may reflect compensatory blood supply to tissue at risk of infarction more accurately than traditional DSC deconvolution analysis (global-AIF). Using a standard MRI acquisition sequence in a preclinical animal model of ischemic stroke, we postprocessed DSC with both 1) a traditional global-AIF,<sup>11</sup> and 2) an automatically generated voxel-wise “local-AIF” that corrects for delay and dispersion of the contrast bolus within every voxel. We hypothesized that quantification of perfusion calculated with an appropriate local-AIF would correlate with the degree of collateral supply to a perfusion bed distal to an occlusion and better predict infarct growth.

## MATERIALS AND METHODS

### Experimental Protocol

All experiments were conducted by using a preclinical canine model of ischemic stroke.<sup>5,9,12-14</sup> The 2-day experimental protocol was approved by the University of Chicago Institutional Animal Care and Use Committee and reported in compliance with ARRIVE guidelines. In this study, a series of 7 purpose-bred adult canines (mean age = 4.1 ± 2.9 years; mean weight = 25.8 ± 3.7 kg; 6 female, 1 male) underwent permanent endovascular middle cerebral artery occlusion (MCAO) via embolic occlusion coils at the M1 segment proximal to the bifurcation (Online Supplemental Data). Subjects underwent x-ray arteriography, MRI DSC perfusion, and serial quantification of infarct volume by DTI and were euthanized either the same evening or the following day.

### Pial Collateral Score via X-Ray Arteriography

Collateral supply was quantified 30 minutes post-MCAO by assessing x-ray arteriographic images (OEC9800; GE Healthcare) with a pial collateral score (PCS).<sup>13-15</sup> PCS is an ordinal score from 1–11

developed for this preclinical model from a score of 1–5 for humans.<sup>15</sup> The scores were evaluated blinded to MRI qCBF by a neurointerventional radiologist with over 20 years of experience with human angiography and over 15 years with angiography in this canine model. Scoring was based on the delay and extent of retrograde filling of arterial branches distal to the occluded artery, with 1 being minimal/no collateralization and 11 being retrograde reconstitution of the collateral network up to the occlusion (Online Supplemental Data). Subjects with PCS ≤8 were considered “poor,” and PCS ≥9 considered “good” collateral supply, determined by a previous study showing “poor” collaterals with core infarct growing rapidly by assessment at the 2-hour time point and “good” collaterals still having a large volume of tissue-at-risk.<sup>14</sup>

### MR Acquisition

All MRI scans were performed on a 3T MRI scanner (Ingenia Philips) with canines in a head-first, prone position by using a 15-channel receive-only coil. DSC perfusion images were acquired 2.5 hours after occlusion (2D gradient-echo, T2\*-weighted EPI, FOV = 160 × 160 mm/matrix = 176 × 176, 5 slices/6 mm thick, TR/TE = 500/30 ms, 120 phases, total scan time = 60s). Rapid, 15-second T1 maps were acquired by using a 2D inversion recovery look-locker scan with a single-shot EPI readout (slice thickness = 6 mm, FOV = 160 × 160 mm/matrix = 176 × 176) for the T1-bookend method. Gadolinium (Gd)-based contrast agent (Multihance, Bracco) was injected in the forepaw, followed by a saline flush (Gd: 3 mL at 2 mL/s, saline: 20 mL at 2 mL/s).

DTIs were acquired at 30-minute intervals to calculate mean diffusivity (MD) post-MCAO for measuring infarct volume growth over time. A stack of 50 2D DTI was prescribed to cover the entire head (slice thickness = 2 mm, FOV = 128 × 128 mm/matrix = 128 × 128, TR/TE = 2993/83 ms, flip angle = 90°, b-values = 0, 800 seconds/mm<sup>2</sup>, 32 directions). MD, rather than ADC, maps were used as DTI was acquired to study separate aspects of this model beyond the scope of the current study; for the purposes of detecting infarct in this study, the sequences are treated as equivalent.

### Traditional Global-AIF DSC Postprocessing

For traditional DSC, the single global-AIF was chosen automatically based on a simultaneous assessment of early arrival time, narrow

bolus, and large area under the concentration curve.<sup>16</sup> qCBF was calculated by using the T1-bookend method<sup>17</sup> where T1 (in ms) changes in the parenchyma and blood pool are input to a 2-compartment model<sup>18-20</sup> that yields qCBF (in mL/100 g/min) including intra- to extravascular water exchange.<sup>19</sup> This T1-bookend method has undergone extensive validation,<sup>9,10,21</sup> is fully automated to minimize user bias,<sup>20</sup> and is available for use.<sup>22,23</sup> Deconvolving the voxelwise parenchymal tissue curves against the global-AIF yields mean transit time values for the calculation of qCBF by using the central volume principle,

$$qCBF(mL/100g/min) = \frac{qCBV(mL/100g)}{MTT(min)}$$

In the remainder of this manuscript, we refer to these values as “global-AIF qCBF” with Tmax calculated as the time at which the residue function reaches its maximum after deconvolution with the global-AIF.<sup>24</sup>

### Local-AIF DSC Postprocessing

In a setting of vascular occlusion, the traditional global-AIF as a global estimate of the contrast bolus shape as it enters the brain has been shown to overestimate the degree of hypoperfusion in vascular beds fed via collateral supply.<sup>11</sup> To address this shortcoming, a local-AIF was automatically generated for every voxel within the deconvolution analysis of DSC perfusion to yield a map of qCBF in mL/100 g/min. This local-AIF was calculated by using a previously reported technique,<sup>10</sup>

$$Local-AIF(t) = Global-AIF(t) \otimes \frac{\alpha}{(\Delta t + 1)} e^{-\frac{\beta t}{\Delta t}}$$

which includes correction for delayed arrival time ( $\Delta t$ ) and bolus dispersion ( $\otimes e^{-\frac{\beta t}{\Delta t}}$ ) before arrival in the vascular bed from comparison between global-AIF and venous outflow (Online Supplemental Data). The local-AIF is patient-dependent, has been previously validated<sup>9,10,21</sup> in humans, and is available for use.<sup>22,23</sup> A prior study supports the local-AIF accounting for both antegrade flow through a tight flow-limiting stenosis, cross-filling through the circle of Willis communication, and retrograde blood supply through collateral vascular networks when calculating perfusion.<sup>10</sup>

### Territories of Interest

Three physiologically relevant territories were operationally defined: 1) diffusion-positive core (core infarct), 2) hypoperfused yet viable (tissue-at-risk) in the ipsilateral MCA territory, and 3) contralateral normal hemisphere MCA territory. All territories were defined as being within the MCA territory across 3 consecutive 6-mm coronal slices starting at and posterior to the M1 segment. The core infarct and tissue-at-risk territories were selected by thresholding MD from DTI and Tmax calculated from global-AIF DSC.

Core infarct was defined, as previously reported,<sup>12,13</sup> as MD < 5.7e<sup>-4</sup> mm<sup>2</sup>/s<sup>6</sup>, converted to binary infarction maps, and used to calculate infarct volumes. Infarction maps taken 2.5 hours post-MCAO were co-registered to DSC (Matlab 2021b, MathWorks) for analysis of the perfusion deficit within and around the core infarct.

Tissue-at-risk (ie, the ischemic penumbra) was defined as having prolonged Tmax relative to the global-AIF (Tmax > 1.0 second) but not yet infarcted (ie, MD > 5.7e<sup>-4</sup> mm<sup>2</sup>/s). Tmax<sup>25,26</sup> thresholds for “hypoperfusion” established in larger human brains may not be appropriate in canines. Therefore, this study’s threshold of Tmax > 1.0 second encompassed all tissue potentially at risk with delayed arrival. These global-AIF Tmax maps, minus the binary infarction maps, were applied to both global-AIF qCBF and local-AIF qCBF maps as binary masks to measure qCBF in tissue-at-risk. Contralateral MCA territory was selected on the same 3 slices based on visible anatomic cues. Perfusion beds in the ipsilateral hemisphere that were not “at-risk” or core infarct were not evaluated in the analysis.

### Statistical Analyses

Wilcoxon signed rank test, boxplots, and scatterplots (linear regression and Bland-Altman) were used to compare tissue qCBF as calculated with a global-AIF and local-AIF. Local-AIF qCBF, global-AIF qCBF, and the difference between the 2 ( $\Delta qCBF = local-AIF qCBF - global-AIF qCBF$ ) were correlated against reference standard x-ray angiographic PCS with linear regression and Spearman rank. To examine how relative CBF (rCBF) would be impacted by AIF selection, rCBF was calculated as the ratio qCBF in tissue-at-risk to contralateral middle cerebral artery territory. As robust collateral supply would maintain homeostasis and slow infarct growth, local-AIF qCBF and global-AIF qCBF distal to the occlusion were correlated against infarct growth via linear regression. Local-AIF and global-AIF qCBF were calculated in mL/100 g/min within territories of interest (infarcted, tissue-at-risk, contralateral) and compared via Wilcoxon signed rank test. Wilcoxon rank sum was used to compare local-AIF and global-AIF qCBF in tissue-at-risk for cases with poor collaterals against cases with good collaterals. To investigate potential influence of AIF selection, the difference in quantitative CBV ( $\Delta qCBV = local-AIF CBV - global-AIF CBV$ ) was compared as a function of collateral score.

The bootstrap Z-test was used to estimate effect size for power calculation. All statistical analysis was performed in R (Rstudio 3.6.1, Posit PBC, 2019) and Python 3.11.4 (Anaconda, 2024), with statistical significance determined at the  $P = .05$  level.

## RESULTS

Access to all results, raw images, and tabulated data are available upon request to the corresponding author. Eighty-three percent of the parent study experiments were “successful” and performed to completion, ie, physiologic parameters maintained as planned and no complications such as procedural-related vessel perforation; the success rate improved over time and reached 100% success for the most recent 9 consecutive experiments of the parent study (this current study analyzed only successful controls of the parent study). Representative parametric qCBF maps of a left MCAO were calculated with a global-AIF and a local-AIF for subjects with (Fig 1A, -B) poor collateral supply (PCS = 8) and (Fig 1C, -D) good collateral supply (PCS = 11). The observed differences in qCBF between Fig 1A, -B, as well as between Fig 1C, -D, result exclusively in postprocessing from the choice of AIF (global versus local); identical DSC images and territory ROIs were used for Fig 1A-B and for Fig 1C-D. The corresponding 1-hour infarct

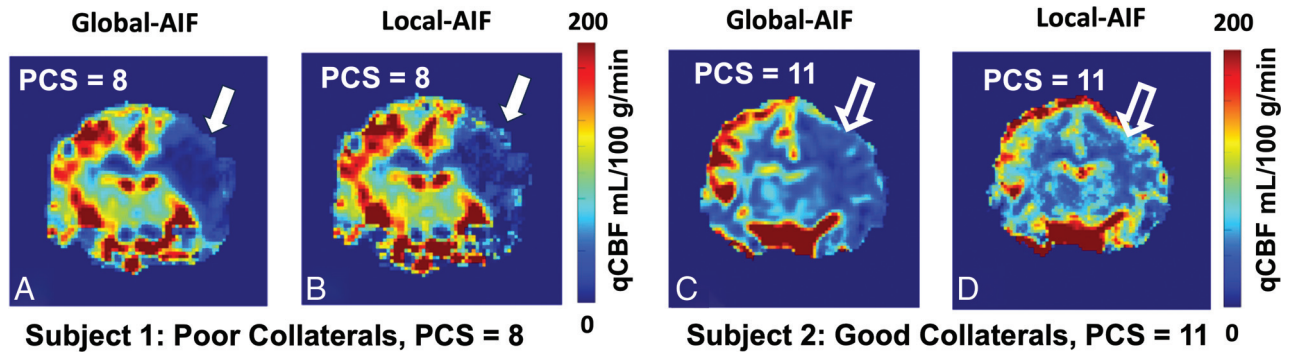


**FIG 1.** Coronal projection parametric qCBF maps in mL/100 g/min. *A*, Poorly collateralized subject (PCS = 8), by using a single global-AIF. *B*, The same subject/images postprocessed by using voxelwise local-AIF. Note the severe hypoperfusion (*deep blue, denoted by arrow*) in the poor collateral supply case, which persists when using a local-AIF. *C*, A subject with robust collateralization (PCS = 11) shown with a global-AIF used to calculate qCBF and (*D*) the same subject/images by using local-AIF to calculate qCBF. Note the markedly higher perfusion values (*hollow, white arrow*) attributable to the use of a delay and dispersed local-AIF.

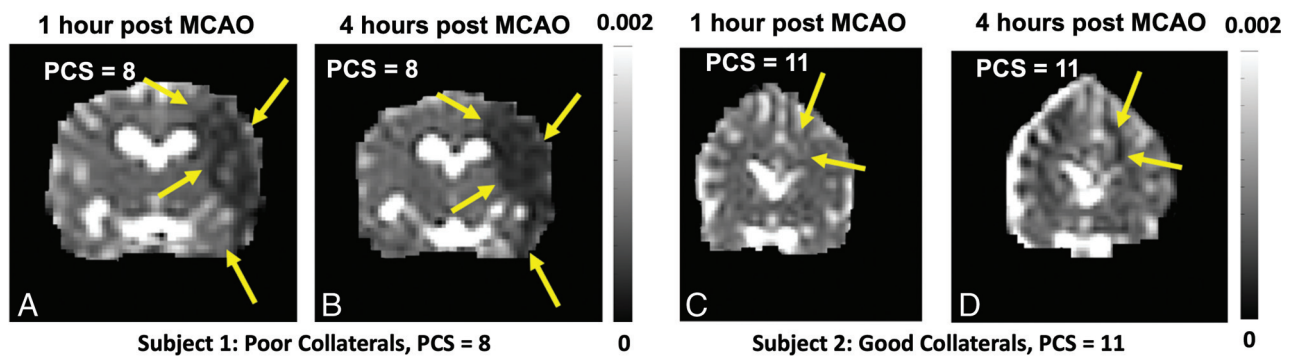


**FIG 2.** Coronal projection parametric mean diffusivity images acquired 1 and 4 hours after coil deployment in the left MCA. These are corresponding diffusion-weighted images from the experiments displayed in Fig 1 with (*A* and *B*) poor collateral supply and (*C* and *D*) good collateral supply. Note that robust collateralization results in significantly slower growing and smaller infarction (*yellow arrows*).

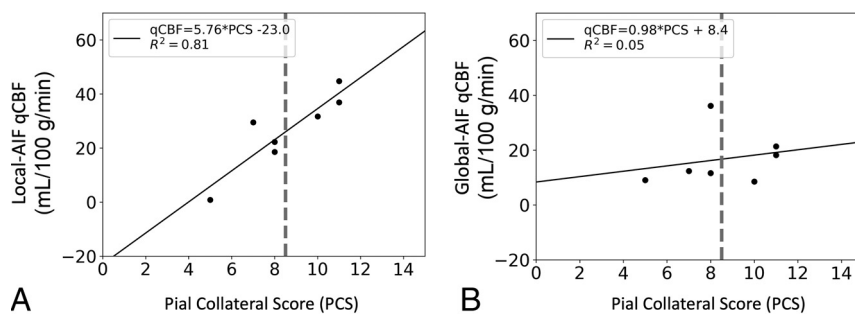


**FIG 3.** Scatterplots of tissue qCBF in mL/100 g/min versus pial collateral score within the operationally defined ischemic penumbra reconstructed with (*A*) a local-AIF and (*B*) a traditional global-AIF. Note: qCBF values are quantitative; values above ~18 mL/100 g/min have sufficient flow to slow infarct growth.

and 4-hour infarct of the 2 cases in Fig 1 are shown in Fig 2 as MD images. Visual inspection of Fig 1 demonstrates that the presence of robust collateral supply (PCS = 11) effectively mitigates the formation and growth of an infarct (Fig 2, *yellow arrows*).

### Collateral Supply

Local-AIF qCBF values in the tissue-at-risk were more strongly correlated (Fig 3A,  $R^2 = 0.81$ ) with PCS than traditional global-

AIF DSC (Fig 3B,  $R^2 = 0.05$ ). This was also true for Spearman rank correlation (local-AIF statistic = 0.87,  $P = .01$ ; global-AIF statistic = 0.34,  $P = .45$ ). The difference between local-AIF and global-AIF qCBF ( $\Delta qCBF = CBF_{LOCAL-AIF} - CBF_{GLOBAL-AIF}$ ) was moderately positively correlated with PCS ( $R^2 = 0.49$ ).

### Infarct Growth

qCBF calculated by using the local-AIF algorithm in the tissue-at-risk was strongly negatively correlated with infarct growth (higher local CBF = slower infarct growth; Fig 4A,  $R^2 = 0.79$ ). In comparison, qCBF values calculated by using a global-AIF were consistently lower than local-AIF values and did not correlate well with infarct growth (Fig 4B,  $R^2 = 0.02$ ).

### Comparison in Territories of Interest

A comparison between traditional global-AIF and delay and dispersion corrected local-AIF qCBF in mL/100 g/min is shown as boxplots in Fig 5. Median qCBF of the core infarct (Fig 5A,

MD  $< 5.7 \times 10^{-4}$  mm<sup>2</sup>/s), tissue-at-risk (Fig 5B, MD  $> 5.7 \times 10^{-4}$  mm<sup>2</sup>/s and Tmax  $> 1.0$  second), and the contralateral hemisphere MCA (Fig 5C) are included. In the infarcted core, both global- and local-AIF showed qCBF values below the threshold for cell death from a study in primates (gray band  $< 18$  mL/100 g/min provided for context to the quantitative value this study calculated).<sup>27</sup> In the tissue-at-risk, the CBF of “good” collaterals (PCS  $\geq 9$ ,  $n=4$ ) and “poor” collaterals (PCS  $\leq 8$ ,  $n=3$ ) is presented separately and color-coded to highlight the sensitivity of the local-AIF to collateral supply (Fig 5B).

A statistical comparison with Wilcoxon signed rank test is shown in the Table. Median qCBF in mL/100 g/min from local-AIF and global-AIF were not statistically significantly different in the core infarct. In the tissue-at-risk, local-AIF and global-AIF were not significantly different for poor collaterals. However, for

good collaterals, local-AIF was higher than global-AIF qCBF by +26.0 mL/100 g/min ( $P = .06$ ), raising the average qCBF above the ischemic threshold. Further, the local-AIF qCBF was an average +25.9 mL/100 g/min higher for subjects with good collaterals compared with local-AIF of poor collaterals (rank sum statistic =  $-2.2$ ,  $P = .03$ ), while global-AIF qCBF of good and poor collaterals were not significantly different (Fig 5B).

### Relative CBF

In the contralateral hemisphere, the local-AIF qCBF was lower for good collaterals by  $-92.5$  mL/100 g/min (rank sum statistic =  $1.9$ ,  $P = .05$ ). In other words, local-AIF showed higher qCBF in tissue-at-risk and lower contralateral qCBF for subjects with robust collateral supply while global-AIF showed lower qCBF in the tissue-at-risk and higher contralateral qCBF. As such, *relative* rCBF = tissue-at-risk/contralateral perfusion with a local-AIF correlated to collateral score ( $R^2 = 0.62$ , Spearman rank statistic =  $0.76$ ,  $P = .04$ ) while global-AIF rCBF did not ( $R^2 = 0.04$ , Spearman rank statistic =  $0.38$ ,  $P = .40$ ). The influence of local-AIF on qCBV was not significant.

### Statistical Power

Regarding power analysis for sample size, difference in the slopes for prediction of infarct growth by using local-AIF (Fig 4A) or global-AIF (Fig 4B) qCBF did not demonstrate statistical

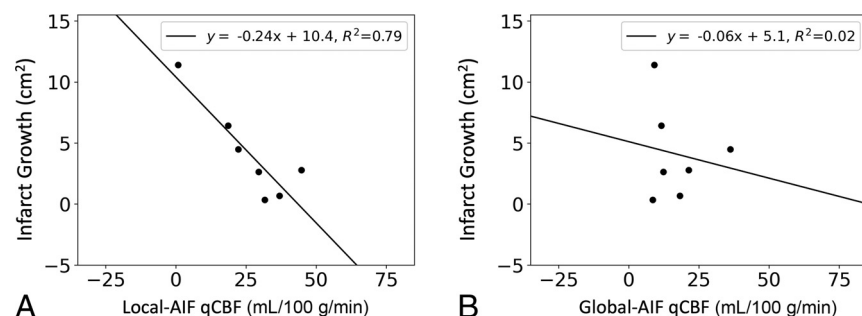


**FIG 4.** In the ischemic penumbra (MD  $> 5.7 \times 10^{-4}$  mm<sup>2</sup>/s, Tmax  $> 1.0$ ) (A) qCBF calculated by using a local-AIF more strongly correlates with slower infarct growth whereas (B) qCBF from a traditionally chosen global-AIF is less predictive of infarct growth in the acute phase of an ischemic stroke.

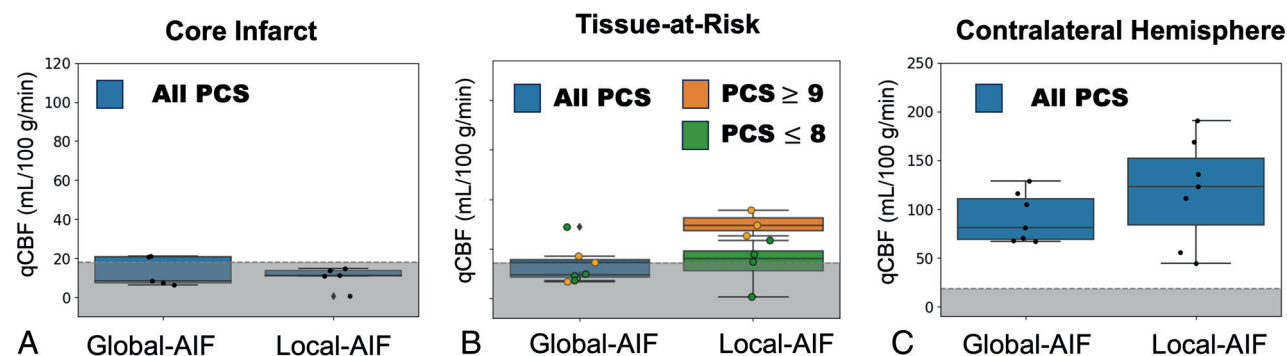


**FIG 5.** Boxplots of CBF in (A) the core of an infarct, (B) the penumbral tissue-at-risk, and (C) the contralateral, unaffected hemisphere. Local-AIF qCBF in tissue-at-risk is separated into good collaterals (PCS  $> 8$ ) and poor collaterals (PCS  $< 8$ ) by color and with scatterplots colored according to score. Contralateral qCBF is in a different range due to systemic compensatory mechanisms to include all data. The gray band represents qCBF values below 18 mL/100 g/min, the ischemic threshold for neuronal death in primates.

### Differences between local-AIF and global-AIF DSC ( $\Delta$ qCBF = local-AIF qCBF – global-AIF qCBF) in the 3 territories of interest, with all collateral scores dichotomized into good and poor<sup>a</sup>

$\Delta$ qCBF Dichotomized by Collateral Score			
Mean Difference (mL/100 g/min) [Wilcoxon signed rank statistic, $P$ value]			
	Core Infarct	Tissue-at-Risk	Contralateral Hemisphere
All PCS	+2.26 [11.0, $P = .68$ ]	+14.3 [5.0, $P = .07$ ]*	-30.06 [16.0, $P = .84$ ]
Good PCS $> 8$	+10.78 [0.0, $P = .125$ ]	+25.96 [0.0, $P = .06$ ]*	-89.2 [2.0, $P = .19$ ]
Poor PCS $< 8$	-9.08 [1.0, $P = .50$ ]	-5.07 [1.0, $P = .50$ ]	+68.60 [1.0, $P = .50$ ]

<sup>a</sup>The underestimation of CBF values by using a single global-AIF compared with a voxelwise local-AIF ( $\Delta$ qCBF) is greater when collateral supply is robust but not significant in a setting of poor collateral supply; this is especially prevalent in tissue-at-risk. Statistical significance at the  $P = .10$  level is denoted with \*.

significance by the bootstrap Z-test ( $Z = -0.49$ ,  $P = .62$ ). However,  $R^2$  values were significantly different ( $Z = 2.03$ ,  $P = .04$ ). In terms of power, the study was underpowered for both end points due to the sample size, with a minimum requirement of 41 subjects for ideal 80% power of both slope and  $R^2$ . However, the trend of improved slope and correlation with a local-AIF remains (Fig 4).

## DISCUSSION

This study found that a voxelwise “local-AIF” that incorporates delay and dispersion of the bolus reflects the existence of compensatory collateral supply distal to an occlusion and predicts infarct growth better than a traditional single global-AIF in DSC MRI. This suggests that a traditional global-AIF without delay and dispersion correction does not include collateral supply and, therefore, may result in a less accurate determination of hypoperfusion when robust leptomeningeal collateralization exists. These findings support the use of a local-AIF to 1) calculate qCBF by using the previously reported “T1 bookend method,”<sup>9,17-21</sup> 2) image CBF supplied through the leptomeningeal arteries, and 3) more accurately predict infarct growth in acute ischemic stroke.

When contrast agent is injected intravenously, it travels through the heart and lungs and finally to the circle of Willis before perfusing the brain. In DSC MRI, the shape of the contrast bolus upon entering the brain represents a global-AIF. However, when there is an occlusion of a major artery, blood will have to travel around the occlusion to reach the infarcted hemisphere through the leptomeningeal collateral arterial network. The delay and the dispersion as blood travels through this collateral network can be corrected for with a local-AIF. The local-AIF presented in this work incorporates a term to account for the late arrival and the additional blunting of the bolus as it is propagated through the brain through the collateral network (Online Supplemental Data). The amount of delayed and dispersed blood that this local-AIF corrects for was hypothesized to be directly related to the extent of collateralization of a subject.

Quantification of local qCBF distal to an occlusion by using a local-AIF demonstrated a strong correlation with the collateralization (ie, PCS). Further, local-AIF qCBF in the tissue-at-risk that would benefit most from robust collateral supply was reported above the threshold of 18 mL/100 g/min for subjects with good collaterals. Meanwhile, in the core infarct, as well as in tissue-at-risk for subjects with minimal collateral supply, local-AIF showed no change in the degree of hypoperfusion. In other words, mathematically, the local-AIF qCBF is the same as the global-AIF qCBF when there is no delayed and dispersed arrival of the bolus through the collateral network ( $Local-AIF_{lim\Delta t \rightarrow 0} = Global-AIF$ ). This supports the automatic local-AIF deconvolution analysis being applicable to all cases, irrespective of collateral supply, delayed antegrade flow, or circle of Willis cross-filling.

Global-AIF qCBF demonstrated poor correlation to collateral supply and no difference between good and poor collaterals, suggesting global-AIF qCBF does not reflect the presence of collateral blood that is supplied, delayed, and dispersed through the leptomeningeal network. The absolute difference between the global-AIF qCBF and the local-AIF qCBF ( $\Delta qCBF$ ) correlated

with PCS, further supporting local-AIF, including the degree of collateral supply (versus slow antegrade stenotic flow) in an ischemic stroke. As both global-AIF and local-AIF use identical input images and regions of interest, the difference was only due to the use of a voxelwise delay and dispersion-corrected local-AIF. The effect of the local-AIF was observed in relative perfusion as well. Local-AIF is an important correction in DSC of acute stroke to include compensatory collateral perfusion distal to an occlusion, even if the intent is for relative perfusion.

A previous study of a perfusion collateral index by Nael et al<sup>28</sup> demonstrated that good collaterals showed smaller volumes of severe hypoperfusion (arterial delay >6 seconds) and larger volumes of moderate hypoperfusion (arterial delay = 2–6 seconds). While severe hypoperfusion with larger arterial delay represents tissue that is not receiving delayed compensatory flow, the moderate arterial delay may represent the delayed and dispersed flow through the collateral network. The current study supports quantifying this collateral supply as qCBF by correction of delay and dispersion with a local-AIF. Further, collaterals from the posterior cerebral artery and anterior cerebral artery territory may have differing timing in the superior and inferior division territories of the occluded MCA; this itself may affect the transit time and lead to qCBF requiring a local-AIF to measure accurately.

Prior studies have reported a correlation between infarct growth from both PCS and arrival time by DSC.<sup>14</sup> The current study provides a mechanistic validation for prior studies by indicating that subjects with higher local-AIF qCBF, which includes contribution from collateral supply and corrected arrival time, observed slower infarct growth. The local-AIF will improve the prediction of infarction compared with global-AIF as it can more accurately represent the perfusion in the tissue-at-risk, even if the perfusion is being supplied, delayed, and dispersed through the collateral network. Robust collateralization may have a longer window of treatment, particularly if collateral supply can be therapeutically enhanced, than an ischemic stroke case without robust collateral supply, which must be treated immediately. As such, local-AIF qCBF may be a predictor of infarct growth and provide insight into novel stroke therapeutic treatments.<sup>7</sup>

Tmax, by definition, identifies the presence of delayed bolus arrival as prolonged Tmax and depicts a malignant pattern used in acute stroke triage to identify patients who would benefit from immediate intervention.<sup>1</sup> The goal of this study was to quantify the leptomeningeal supply that mitigates infarct growth. The results suggest that Tmax can identify the *location* of delayed bolus arrival as tissue-at-risk and that a local-AIF can then *quantify* the local flow (ie, degree of collateral supply) from the collateral network in that tissue-at-risk.

A previous study by Federau et al<sup>29</sup> has reported “local perfusion fraction” in acute stroke by using noncontrast intravoxel incoherent motion (IVIM), with excitation and readout in the same plane, as a measure of collateral blood supply that traditional global-AIF DSC cannot capture. This current study demonstrated that traditional global-AIF can be improved by correcting for the delay and dispersion to return the local perfusion. The correlation of local-AIF qCBF to x-ray DSA PCS supported the ability of DSC to quantify “local” collateral supply in mL/100 g/min. In addition, as the influence of a local-AIF on qCBV was not significant, the increased

correlation with a local-AIF was predominately due to the mean transit time component rather than the blood volume component. Since qCBF (in mL/100 g/min) from a combination of the qCBV (with a T1 bookend) and local mean transit time (with a local-AIF) correlated with collateral supply and infarct growth, studies of local IVIM perfusion fraction<sup>29</sup> in acute stroke may benefit from an inclusion of mean transit time to quantify collateral supply.<sup>30</sup>

This work was not without limitations. The use of a complex preclinical animal model limited the number of experiments that were run and vascular territories that were studied. We present a retrospective reanalysis of an animal model that was designed to study flow augmentation in MCAO and was not powered for study of more subtle local- versus global-AIF qCBF differences between groups. This MCAO model and use of contrast afforded a limited number of perfusion measurements; a method that allows dynamic assessment of perfusion over the course of infarct development could be beneficial.<sup>29,30</sup> Coregistration and resampling were required for mapping of core infarct and tissue-at-risk, enabling imperfect coregistration of perfusion and diffusion images; images were analyzed region-by-region, rather than voxel-by-voxel. Translation of conclusions derived from animal-based models is a potential limitation; however, an MCAO model reduces error in evaluating methods for CBF calculation by allowing for a more accurate assessment of occlusion time and comparison of subjects at multiple time points under similar physiologic conditions, which is not possible in humans. The finite number of subjects used in this study limits statistical interpretation and significance. Additional studies are planned and underway in humans to examine translation from a canine model to humans. While the time of reconstruction of local-AIF qCBF maps is not prohibitive and could be incorporated into existing analysis at the scan console, “time-to-needle” constraints remain for clinical use of MRI in acute stroke; the automatic voxelwise local-AIF may have more clinical value as an adaptation in CT perfusion deconvolution.

## CONCLUSIONS

When there is an occlusion of a major artery, the delay and dispersion as blood and contrast travel around the occlusion via the collateral network can be corrected to capture collateral supply with a local-AIF. By using a local-AIF to calculate qCBF, the collateral supply was quantified, correlated with PCS, and predicted infarct growth. These findings support the use of a local-AIF rather than a single global-AIF to 1) calculate qCBF in tissue-at-risk, 2) reduce false hypoperfusion in DSC of large vessel occlusions, and 3) quantify the blood supplied to a compromised perfusion bed through the leptomeningeal arteries. This quantitative local-AIF qCBF may be of benefit to studies of novel stroke therapeutics that would be influenced by collateral supply and for translation to clinical CT perfusion.

Disclosure forms provided by the authors are available with the full text and PDF of this article at [www.ajnr.org](http://www.ajnr.org).

## REFERENCES

1. Liebeskind DS, Saber H, Xiang B; DAWN Investigators, et al. Collateral circulation in thrombectomy for stroke after 6 to 24 hours in the DAWN trial. *Stroke* 2022;53:742–48 [CrossRef Medline](#)
2. Winship IR. Cerebral collaterals and collateral therapeutics for acute ischemic stroke. *Microcirculation* 2015;22:228–36 [CrossRef Medline](#)
3. Marks MP, Heit JJ, Lansberg MG; DEFUSE 3 Investigators, et al. Endovascular treatment in the DEFUSE 3 study. *Stroke* 2018; 49:2000–03 [CrossRef Medline](#)
4. Shazeeb MS, King RM, Anagnostakou V, et al. Novel oxygen carrier slows infarct growth in large vessel occlusion dog model based on magnetic resonance imaging analysis. *Stroke* 2022;53:1363–72 [CrossRef Medline](#)
5. Christoforidis GA, Saadat N, Liu M, et al. Effect of early sanguinate (PEGylated carboxyhemoglobin bovine) infusion on cerebral blood flow to the ischemic core in experimental middle cerebral artery occlusion. *J Neurointerv Surg* 2022;14:1253–57 [CrossRef Medline](#)
6. Saadat N, Christoforidis GA, Jeong YI, et al. Influence of simultaneous pressor and vasodilatory agents on the evolution of infarct growth in experimental acute middle cerebral artery occlusion. *J Neurointerv Surg* 2020;13:741–45 [CrossRef Medline](#)
7. Liu M, Saadat N, Jeong YI, et al. Augmentation of perfusion with simultaneous vasodilator and inotropic agents in experimental acute middle cerebral artery occlusion: a pilot study. *J Neurointerv Surg* 2023;15:e69–75 [CrossRef Medline](#)
8. Lee MJ, Son JP, Kim SJ, et al. Predicting collateral status with magnetic resonance perfusion parameters: probabilistic approach with a Tmax-derived prediction model. *Stroke* 2015;46:2800–07 [CrossRef Medline](#)
9. Jeong YI, Christoforidis GA, Saadat N, et al. Absolute quantitative MR perfusion and comparison against stable-isotope microspheres. *Magn Reson Med* 2019;81:3567–77
10. Mouannes-Srouf JJ, Shin W, Ansari SA, et al. Correction for arterial-tissue delay and dispersion in absolute quantitative cerebral perfusion DSC MR imaging. *Magn Reson Med* 2012;68:495–506 [CrossRef Medline](#)
11. Calamante F, Willats L, Gadian DG, et al. Bolus delay and dispersion in perfusion MRI: implications for tissue predictor models in stroke. *Magn Reson Med* 2006;55:1180–85 [CrossRef Medline](#)
12. Rink C, Christoforidis G, Abduljalil A, et al. Minimally invasive neuroradiologic model of preclinical transient middle cerebral artery occlusion in canines. *Proc Natl Acad Sci U S A* 2008;105:14100–05 [CrossRef Medline](#)
13. Christoforidis GA, Rink C, Kontzialis MS, et al. An endovascular canine middle cerebral artery occlusion model for the study of leptomeningeal collateral recruitment. *Invest Radiol* 2011;46:34–40 [CrossRef Medline](#)
14. Christoforidis GA, Vakil P, Ansari SA, et al. Impact of pial collaterals on infarct growth rate in experimental acute ischemic stroke. *AJNR Am J Neuroradiol* 2017;38:270–75 [CrossRef Medline](#)
15. Christoforidis GA, Mohammad Y, Kehagias D, et al. Angiographic assessment as a prognostic indicator following intra-arterial thrombolysis for acute ischemic stroke. *AJNR Am J Neuroradiol* 2005;26:1789–97 [Medline](#)
16. Carroll TJ, Rowley HA, Haughton VM. Automatic calculation of the arterial input function for cerebral perfusion imaging with MR imaging. *Radiology* 2003;227:593–600 [CrossRef Medline](#)
17. Carroll TJ, Horowitz S, Shin W, et al. Quantification of cerebral perfusion using the “bookend technique”: an evaluation in CNS tumors. *Magn Reson Imaging* 2008;26:1352–59 [CrossRef Medline](#)
18. Sakaie KE, Shin W, Curtin KR, et al. Method for improving the accuracy of quantitative cerebral perfusion imaging. *J Magn Reson Imaging* 2005;21:512–19 [CrossRef Medline](#)
19. Shin W, Cashen TA, Horowitz SW, et al. Quantitative CBV measurement from static T1 changes in tissue and correction for intravascular water exchange. *Magn Reson Med* 2006;56:138–45 [CrossRef Medline](#)
20. Shin W, Horowitz S, Ragin A, et al. Quantitative cerebral perfusion using dynamic susceptibility contrast MRI: evaluation of reproducibility and age- and gender-dependence with fully automatic image postprocessing algorithm. *Magn Reson Med* 2007;58:1232–41 [CrossRef Medline](#)
21. Vakil P, Lee JJ, Mouannes-Srouf JJ, et al. Cerebrovascular occlusive disease: quantitative cerebral blood flow using dynamic susceptibility contrast MR imaging correlates with quantitative H2[15O] PET. *Radiology* 2013;266:879–86 [CrossRef Medline](#)

22. Systems SM. **Absolute quantitative DSC cerebral perfusion imaging with SCALE-PWI.** *N4\_VD13D\_1049\_Z00387MF\_QIAN\_SCALEPWI*. 2015;WIP #1049.
23. *T1Bookend DSC Perfusion with Global and Local AIF Open Source Code [computer program]*. Version 1.2.0. Github 2024
24. Shah MK, Shin W, Parikh VS, et al. **Quantitative cerebral MR perfusion imaging: preliminary results in stroke.** *J Magn Reson Imaging* 2010;32:796–802 [CrossRef Medline](#)
25. Yaghi S, Khatri P, Prabhakaran S, et al. **What threshold defines penumbral brain tissue in patients with symptomatic anterior circulation intracranial stenosis: an exploratory analysis.** *J Neuroimaging* 2019;29:203–05 [CrossRef Medline](#)
26. Calamante F, Christensen S, Desmond PM, et al. **The physiological significance of the time-to-maximum (Tmax) parameter in perfusion MRI.** *Stroke* 2010;41:1169–74 [CrossRef Medline](#)
27. Jones TH, Morawetz RB, Crowell RM, et al. **Thresholds of focal cerebral ischemia in awake monkeys.** *J Neurosurg* 1981;54:773–82 [CrossRef Medline](#)
28. Nael K, Doshi A, De Leacy R, et al. **MR perfusion to determine the status of collaterals in patients with acute ischemic stroke: a look beyond time maps.** *AJNR Am J Neuroradiol* 2018;39:219–225 [CrossRef Medline](#)
29. Federau C, Wintermark M, Christensen S, et al. **Collateral blood flow measurement with intravoxel incoherent motion perfusion imaging in hyperacute brain stroke.** *Neurology* 2019;92:e2462–71 [CrossRef Medline](#)
30. Liu M, Saadat N, Jeong Y, et al. **Quantitative perfusion and water transport time model from multi b-value diffusion magnetic resonance imaging validated against neutron capture microspheres.** *J Med Imaging (Bellingham)* 2023;10:063501 [CrossRef](#)